An anode composition influence on the efficiency of producing sodium ferrate for metallurgical plants wastewater treatment

A. P. Petkova, *Dr. Eng., Prof.* [1]*, e-mail: apetkova@inbox.ru;*
A. I. Konyashina, *General Director* [2]*, e-mail: akoniashina@ya.ru;*
G. R. Sharafutdinova, *Postgraduate Student* [1]*, e-mail: grsharafutdinova@yandex.ru;*
O. Yu. Ganzulenko, *Cand. Eng., Associate Prof.* [1]*, e-mail: oxana_ganza@mail.ru*

[1] *Empress Catherine II Saint Petersburg Mining University (St. Petersburg, Russia)*
[2] *"Dobrokhim" LLC (Saint-Petersburg, Russia)*

The article investigates the electrochemical synthesis of sodium ferrate using anodes made of ferritic steel alloyed with silicon concentrations of 4.15 %, 5.5 %, 6.8 % and 7.5 %. It has been found that silicon content increase in the anodes contributes to a significant improvement in the basic parameters of the process. With silicon content of 7.5 %, the maximum concentration of sodium ferrate in solution was reached – up to 18 g/dm^3, which is 3 times higher than with transformer steel anodes, while increasing productivity and reducing specific energy consumption for synthesis. The increased silicon content facilitates the destruction of the oxide film on the surface of the anode in alkaline solution, which slows down electrochemical processes, which makes it possible to stabilize the reactor's efficiency for a long time. Sodium ferrate demonstrates high efficiency in removing heavy metals, organic compounds, and fine particles from wastewater generated by mining and metallurgical plants. These data confirm the possibility of using sodium ferrate for the purification of the process waters used in the processing of non-ferrous ores and rare earth metals, as well as to prevent negative effects on the environment.
Key words: wastewater from metallurgical enterprises, sodium ferrate, electrochemical process, reactor, sacrificial anode, electrolyte.
DOI: 10.17580/cisisr.2025.01.19

Introduction

Generated during the processing of metal ores wastewater contains high concentrations of heavy metals, fine solid particles and organic chemical compounds. Such pollutions are caused by the complex composition of the processed minerals, the used enrichment methods and the usage of large chemical reagents number [1–3]. These waters pose a significant danger to the environment due to their toxicity and the complexity of their composition makes the purification an important environmental problem. Modern research confirms the importance of developing waste recycling methods aimed at reducing their environmental influence [4–6]. Therefore, an urgent task is to find the cheap and environmentally friendly technologies for wastewater treatment without chlorine-containing reagents which are not inferior in efficiency and cost to the technologies with hypochlorite (chlorine), as well as solving the problem of meeting the requirements for the wastewater purity without using chlorine [7].

One of the promising reagents for a wastewater treatment is sodium ferrate (Na_2FeO_4) [8–10]. Due to its high oxidizing and coagulating properties, sodium ferrate effectively removes organic pollutants, heavy metals and microorganisms [11–13]. For example, its application on water of the Krasny Bor liquid toxic waste landfill in St. Petersburg demonstrated the possibility of the significantly reducing concentration of such heavy metals as Cd and Pb from exceeding the MPC requirements respectively by more than 2,000 and 100 [14]. In addition, when ferrates disintegrate during an oxidation, they form iron hydroxides, which exhibit the more effective coagulation compared to ferrous sulfate, ferric nitrate, ferric chloride and aluminum sulfate, accelerating the pollutants precipitation [14]. These properties make ferrates particularly suitable for the treating difficult effluents, including acid mine waters [15, 16].

Studies show that sodium ferrate achieves almost complete removal of most metals, including iron, magnesium, cobalt, copper, sodium and nickel, with 99–100 % efficiency. However, cadmium removal was less efficient in low pH samples due to its solubility properties. When pH increased, cadmium removal efficiency increased significantly. This observation was confirmed by experiments on acid mine waters collected from several plots in the Johannesburg and Pretoria regions of South Africa [16].

In addition to heavy metal removal, sodium ferrates have strong oxidizing and bactericidal properties, what expands their application in wastewater treatment. They are effective in breaking down organic pollutants, including phenols, and have the ability to destroy a wide range of microorganisms, including bacteria and viruses [17, 18]. These properties make sodium ferrates particularly suitable for the complex treatment of wastewater with high organic and pathogenic microorganism content, such as solid waste landfill filtrates [19].

© A. P. Petkova, A. I. Konyashina, G. R. Sharafutdinova, O. Yu. Ganzulenko, 2025

The importance of developing new wastewater treatment methods is also confirmed by the results of studies carried out Sredneuralsk Copper Smelter (Revda) and Kirovgrad Hard Alloy Plant (Kirovgrad). The wastewater removal efficiency using arsenic ferrate at Sredneuralsk copper smelter reached 100%, and wastewater of Kirovgrad hard alloy plant was purified from tungsten with an efficiency of 99.2 % [20].

Taking into account the high efficiency of sodium ferrate, the key direction of research is increasing its concentration in the produced solution. While ferrate concentration increase the required dose of the reagent introduced into the treated water is proportionally reduced. This allows us to reduce the alkalinity, pH of the treated wastewater and effectively purify water with high COD and BOD values. At the same time, alkali and energy consumption and the overall cost of ferrate production as well are reduced. Reducing costs and improving the environmental friendliness of such processes play a key role in making wastewater treatment technologies available for industrial applications. So, this reliable and long-term operation of industrial equipment involved in cleaning processes, is a paramount importance [21].

Since the anode is the main source of iron and ensures process stability, its composition remains a relevant area of research. Therefore, a special attention should be paid to the effect of the consumable anode composition on the ferrate concentration in the solution, the productivity and energy consumption of the electrolysis process. Papers [22–23] examined the influence of the steel and cast iron anodes composition on the productivity of the electrolysis process and the concentration of ferrate, among them researches devoted to the study of the silicon role in the composition of consumable anodes were of particular interest. Alloying anode with silicon improves the material's resistance to corrosion and prevents its passivation during the long-term electrolysis, which helps to increase the efficiency of the sodium ferrate synthesis and reduces the energy costs [24–26]. However, there are no systematic studies of the silicon content influence on the anodes structure and properties, on the performance of the electrolysis process and the concentration of ferrate in the solution, what is the one of this study objectiveIn addition, adaptation methods research and efficiency of equipment improving in industrial enterprises emphasizes the importance of a well-considered choice of materials and technical solutions [27–29].

Therefore, the aim of the presence work is to study the anode composition influence on the increase of sodium ferrate concentration in the produced solution, proportionally to which concentration the required dose of sodium ferrate decreases, and the efficiency of cleaning wastewater with high values of chemical and biological contaminants increases.

Materials and methods of research

Flow production of sodium ferrate was carried out in a membrane electrochemical reactor, as electrolyte was 20 % NaOH solution. The electrolyte choice provided low electrical resistance, reduced energy consumption, increased membrane durability and significant ferrate cost reduction compared to analogues produced in solutions with an alkali concentration of 40–60 %. The cathodes were made of X10CrNiTi18-9 austenitic steel, it is resistant to alkali and sodium ferrate, and as the membrane was used the cation exchange membrane Nafion-324. The reactor housing was manufactured by means of 3D-printing technology for creating a scalable design [30, 31]. Polypropylene was chosen as the reactor material, which has high chemical resistance in an alkaline solution and at the obtaining concentrations of sodium ferrate. To reduce shrinkage and deformation of the housing, polypropylene thread of grade Nova PPGF, it was reinforced with short glass fiber, what increased strength and rigidity of the reactor housing [32]. The reactor housing was printed on "Sapphire S" 3D-printer, manufactured by Two Trees. The nozzle temperature was 270 °C, the table temperature was 95 °C. The layer thickness was 0.2 mm with a nozzle diameter of 0.8 mm. The choice of materials which can withstand aggressive operating conditions allows us to increase reliability and efficiency of the equipment [33–35].

As in the previous version of the reactor composition [14], the final version of it implements a flow reactor (**Fig. 1**, *a–c*) with one anode, two cathode chambers to the left and right of it and a side chamber for collecting ferrate (Fig. 1, *a*, *b*). The side chamber contains a built-in photometric sensor for the ferrate concentration measuring in an alkali solution, described in detail in [31].

Particular attention was paid to the anodes selection, as they are a key component determining the process productivity [36–38]. The base material was mass-produced hot-rolled thin-sheet electrical ferrite steel, grade 1512, with a silicon content of 4.15 % and a thickness of 0.5 mm (Fig. 1, *d*). Since ferrite transformer steels contain from 3.8 to 4.8 % of silicon, in order to test the silicon content effect on ferrate concentration and process productivity, there were

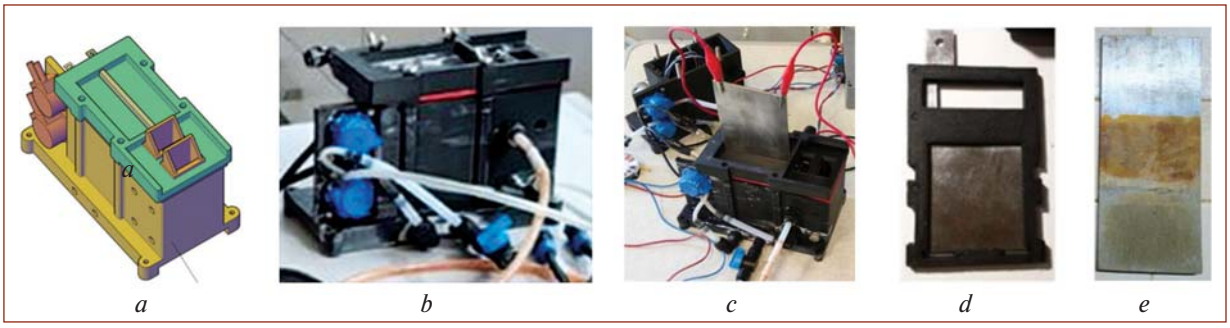

Fig. 1. The construction (*a*) and the appearance of the reactor (*b, c*) and anodes (*d, e*)

smelted, rolled and cut to size for electrodes samples containing 5, 6 and 7% of silicon (Fig. 1, *e*).

To clarify the calculated anodes chemical composition there was analyzed the silicon content by scanning electron microscopy together with energy-dispersive X-ray spectroscopy (SEM-EDS) on Zeiss – Supra 40VP scanning electron microscope (**Table 1**). The studied ferrite low-carbon steels are characterized by carbon content from 0.02 to 0.06 %. The main component is iron (Fe) with the mass fraction of 92.51 to 94.54 %, and the silicon (Si) content varies from 5.46 to 7.49 %. In addition, there was determined the impurities content for one of the samples using optical emission spectral analysis (AESA) by optical emission spectrometer "Iskroline-100" (Table 1). **Fig. 2** shows the results of X-ray structural analysis (XRD) for the anodes, performed with Bruker X-ray diffractometer "D8 Advance".

During scanning samples on X-ray diffractometer there were detected the superstructural peaks near 37° for the samples containing 6.8 % Si (sample 6) and 7.5 % Si (sample 7, Fig. 2, *a*) in addition to the peaks corresponding to α-Fe for the sample 5 with 5.5 % Si. The scanning was carried out using cobalt radiation. No superstructural peaks were detected in the sample 5. For all samples, the peaks were detected at the same angles, indicating presence of silicon in a solid solution of α-Fe and in the form of iron silicide as well. The silicon content increase in the solid solution indicates also on the lattice period enlargements in the samples 5, 6 and 7, which are amounted up to 2.856, 2.858 and 2.859 Å respectively. The parameters of the α-Fe samples bcc lattice unit cells were determined by refining the full profile with the XRD patterns using the Rietveld method with SmartLab software.

Metallographic analysis of the amount, size and location of iron silicide in ferrite matrix was carried out an inverted optical microscope IM7200 MEIJI TECHNO with Thixomet image analyzer software. The size and the quantity of silicide grows with silicon content increasing, they are located both at the boundaries and fairly uniformly within the ferrite grains (Fig. 2, *b–d*). According to the state diagrams [39], the ferrite steels embrittlement takes place due to iron silicide formation of Fe6Si type with the silicon content increase up to 6.5–7.5 %. Electrode ingots with increased silicon content were rolled to the thickness of 3 mm, designed for three days continuous operation.

Results of the experiment

To find out the influence of the anode composition on the ferrate concentration, current efficiency and energy consumption of the process, there were manufactured four anode variants containing different amounts of silicon. The

Table 1. Chemical composition of the electrodes

Sample	Method	Fe,%	C,%	Cr,%	Cu,%	Mn,%	P,%	S,%	Si,%	Al,%
1512	SEM	95.52	–	–	0.28	–	–	–	4.15	0.05
5	SEM	94.54	–	–	–	–	–	–	5.46	–
6	SEM	93.17	–	–	–	–	–	–	6.83	–
7	SEM	92.51	–	–	–	–	–	–	7.49	–
6	AESA	Res.	0.06	0.03	0.005	0.02	0.005	0.007	6	0.007

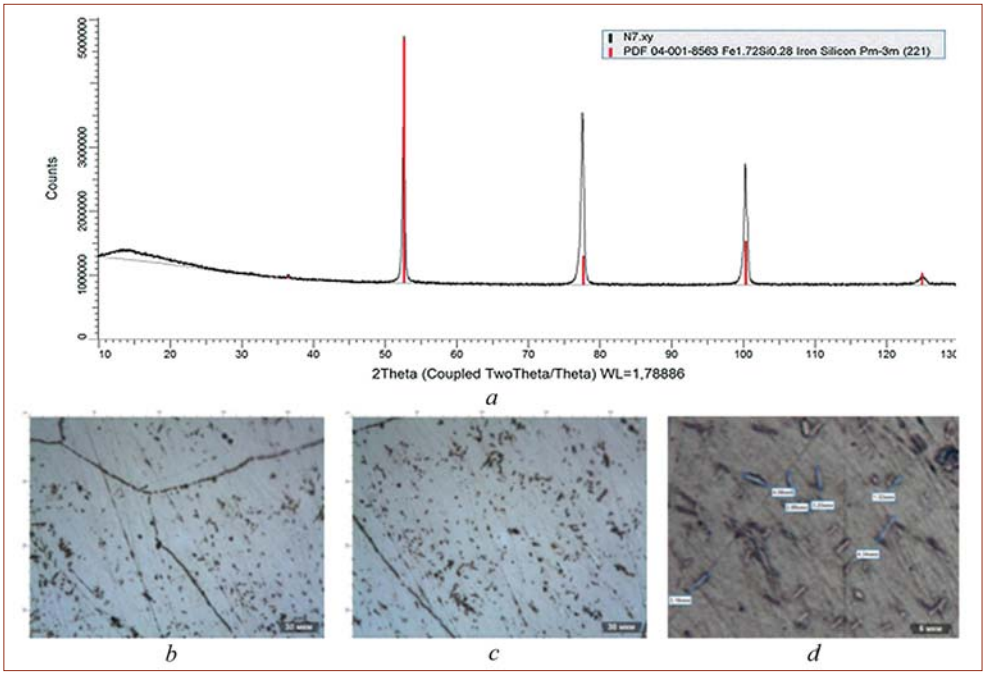

Fig. 2. XRD results (*a*) and metallographic analysis (*b–d*) for the sample 7 with 7.5 % Si

first anode was laser-cut from a sheet of hot-rolled ferritic transformer steel grade 1512 and 0.5 mm thickness, containing 4.15 % silicon, and placed in a quick-release polypropylene frame (Fig. 1, *d*). Three other anode variants were rolled and cut to size from specially smelted ingots containing 5.5, 6.8, and 7.5 % silicon (Fig. 1, *e*). The mass of each ingot was 5 kg, after removing the bottom and top parts of them they were rolled into electrodes under the heating temperature for rolling of 1250–1260 °C and the end of rolling at temperatures of no lower than 800–900 °C. There were obtained 3 blanks from each ingot, 2 electrodes from each blank with a thickness of 3 mm were cut.

With a silicon content of 5.5–7.5 %, either ingot iron or ferrite with iron silicide inclusions is formed, which causes embrittlement of the material and deterioration of deformability during the rolling process. It is assumed that the silicon content increasing in the anode enhances its corrosion resistance in the atmosphere and facilitates easier destruction of the oxide film on the surface in an alkaline environment during an electrochemical reaction, which ensures better anode decomposition and the electrolysis process stability.

Four series of experiments were carried out using steel anodes with silicon contents of 4.15 %, 5.5 %, 6.8 % and 7.5 %. The process was done without recirculation for the first 15 minutes, after that the electrolyte was renewed with the rate of 3 ml/min. Samples for analysis were taken in 45 minutes after beginning of each experiment, that made it possible to study the silicon content effect in the anodes on the rate of sodium ferrate formation and its concentration.

Fig. 3 shows the relationships of the ferrate concentration in the solution (*a*), the productivity of the electrolysis process (*b*) and the energy consumption (*c*) on the silicon content in the anode after 45 minutes of electrolysis. The productivity of the sodium ferrate synthesis was calculated based on its yield relative to the maximum theoretical current yield, which is determined according to Faraday's law. The iron decomposition rate according to Faraday was 1.6 g/h. It is evident that the concentration of sodium ferrate increases proportionally to the silicon content increase in the anode (Fig. 3, *a*). The productivity of the electrolysis process, determined by the current yield, reflecting the efficiency of using electric current to form sodium ferrate, also increases proportionally to the silicon content increase in the anode (fig. 3, *b*). At the same time, the specific energy costs for the sodium ferrate production decrease proportionally to the silicon content increase in the anode (fig. 3, *c*).

The silicon content increase in the anode from 4.15 % to 7.5 % rises the electrochemical synthesis productivity of sodium ferrate. This is expressed in the concentration ferrate increase, the energy consumption decrease and the current yield increase. The positive silicon effect on the ferrate synthesis process is associated with the oxide film stability decrease in an alkaline environment due to the selective (chemical and electrochemical) dissolution of silicon from the surface layer of silicide, as a result of which the decomposition of the anode during electrolysis is facilitated, energy for side processes losses so as anode oxidation or oxygen release are reduced.

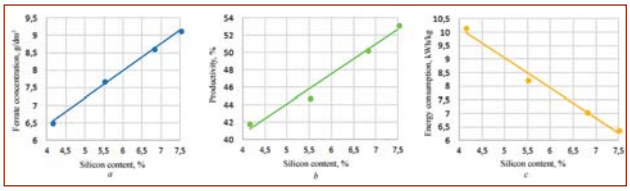

Figure 3. Relationships of sodium ferrate concentration (*a*), electrolysis process productivity (*b*) and energy consumption (*c*) on the silicon content in anode

For the long-term experiment thee were selected the anodes with a silicon content of 7.5% so as they provided the highest sodium ferrate concentration and the best productivity in short-term tests. The voltage and sodium ferrate concentration readings were recorded throughout the experiment. The readings were recorded in 45 minutes after the experiment beginning, then every 15 minutes for two hours, then every hour for seven hours, and then every three hours. When the sodium ferrate concentration decreased, the readings were recorded again every hour until the end of the experiment. **Fig. 4** shows the relationships of the sodium ferrate concentration (*a*) and the productivity (current yield) of the electrolysis process (*b*) during long-term tests.

The decrease of sodium ferrate concentration is due to the anode degradation at the last stages of the experiment. This process leads to deterioration of its electrochemical characteristics and decreases the synthesis efficiency. **Fig. 5**, a shows the anode in 69 hours after the experiment beginning, where stratification and destruction of the surface are noticeable. Fig. 5, *b* shows the state of the anode after 70 hours of sodium ferrate production. These visual changes confirm the observed decrease in the productivity of the process and an increase in the voltage on the cell.

The increased silicon content in the anode prevents the oxides film formation on the surface and their passivation during long-term electrolysis, that makes it possible to increase the ferrate concentration of the solution in flow pro-

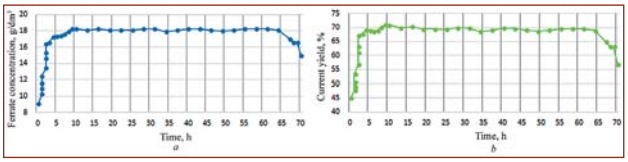

Fig. 4. Relationships of the sodium ferrate concentration (*a*) and the electrolysis process productivity (current yield) (*b*) on time

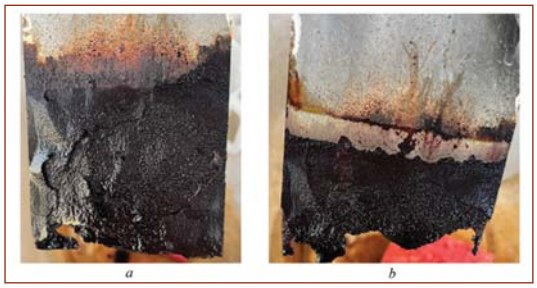

Fig. 5. Anode in 69 hours (*a*) and in 70 hours (*b*) after experiment beginning

duction comparing to 1512 steel transformer electrodes from 6 to 18 g/dm^3, the process productivity up to 70 % and to ensure stable operation of the reactor up to the anodes destruction in 70 hours of continuous operation.

Discussion of the results

According to available literature data and as a result of volt-ampere response research, it was established [40] that, due to silicon presence in anode, its electrochemical activity increases in several times when comparing the electrical steels grades up to 3 % of silicon content in the area of transpassive potential and ingot iron or low-carbon steels. This leads to an easier process of transpassive oxidation for steels with a high silicon content compared to ingot iron and low-carbon steels, as well as an easier oxidation of Fe(III) to Fe oxides of higher valence.

Due to the overpotential reduction of the ferrate (VI) formation reaction which coming out ferrate (VI) by chemical disproportionating (1, 2), this reaction takes priority over the oxygen evolution reaction (3) at higher anodic potentials, and thus the efficiency of ferrate (VI) increases. This leads to a significant increase in the efficiency of ferrate(VI) under identical process conditions [37].

$$FeOOH + 3OH^- \rightarrow FeO_3^{2-} + 2H_2O + e^- \quad (1)$$

$$3FeO_3^{2-} + H_2O \rightarrow 2FeO_2^- + FeO_4^{2-} + 2OH^- \quad (2)$$

$$2OH^- \rightarrow H_2O + {}^1/_2O_2 + 2e^- \quad (3)$$

In the manufactured anodes with the silicon content increase in steel up to 7.5 % the dispersed iron silicides formation of the approximate composition Fe6Si are observed (Fig. 2, *a*), which are distributed both along the grain boundaries and inside them (Fig. 2, *b*, *c*). With the silicon percentage increase from 6.8 to 7.5 %, the number of these silicides increases significantly. They have more negative electrochemical potential than α-Fe, which causes their selective oxidation and dissolution in an alkaline medium (pH > 14), thereby increasing the area of the active surface of the anode, its porosity and permeability of the oxide film. The porous oxide-hydroxide layer allows hydroxide ions (OH^-) to penetrate faster to the fresh metal surface, which accelerates the transpassive dissolution process of the anode. This helps to avoid premature passivation of the anode and increases the efficiency of electrochemical synthesis of ferrate (VI) in long-term experiments. The porous oxide-hydroxide layer allows hydroxide ions (OH^-) to penetrate faster to the fresh metal surface, which accelerates the transpassive dissolution process of the anode. This helps to avoid premature passivation of the anode and increases the efficiency of electrochemical synthesis of ferrate (VI) while doing the long-term experiments.

In addition, the silicon dissolution from α-Fe crystals can be proceeded via the silicate anions formation of such as $HSiO_3^-$ or SiO_3^{2-}, which then either freely diffuse in the electrolyte or polymerize to form a silicate gel on the membrane or anodes. This gel, adsorbing on iron (III) hydroxide, helps to maintain the porosity and permeability of the oxide-hydroxide layer. Thus, the active surface of the anode is preserved until its destruction, ensuring the efficiency of the electrochemical synthesis process of ferrate (VI).

Conclusion

A rational choice of the material for the consumable anode is substantiated and demonstrated in this paper. The choice provides high values of sodium ferrate concentration in the solution, productivity and duration of the process. Increasing the silicon content in the anodes from 4.15% to 7.5% contributed to increase the sodium ferrate concentration in the solution by up to 1.5 times during short-term and up to 3 times during long-term electrolysis, while increasing productivity and reducing energy costs of the process.

The silicon content increase in the composition of iron-silicon anodes leads to a sharp increase in their electrochemical activity in the area of transpassive dissolution and ferrate (VI) formation. Quantitatively, this is expressed in an increase of the ferrate concentration in the solution with an increase in the silicon content under the same experimental conditions (Fig. 3). The significantly higher surface activity of steels with high silicon content facilitates the formation of ferrate at voltage close to the competing oxygen evolution voltage. The stability of the long-term electrolysis process is due to the local selective destruction of the passivation layer and the formation of a porous oxide-hydroxide layer formed on the iron-silicon anodes. This is a consequence of the dispersed iron silicides presence in α-iron (with 6.5–7.5 % Si) or the presence of Si in α-iron solid solution at a lower content (4.15–5.5 %), which ensures selective oxidation and dissolution of anodes, an increase in the area of their active surface and an increase in the porosity and permeability of the oxide film. Increasing the silicon content in consumable anodes from 4.15 to 7.5 % is an effective method to maintain the stable reactor operation and efficient production of ferrate (VI) under the long-term continuous electrolysis conditions. In addition, it allows to obtain a comparable concentration of ferrate in an alkaline solution with a NaOH concentration of 5 M compared to significantly more concentrated solutions of 14–16 M.

REFERENCES

1. Meng S., Wen S., Han G., Wang X., Feng Q. Wastewater treatment in mineral processing of non-ferrous metal resources: a review. *Water*. 2022. Vol. 14. No. 5. p. 726. DOI: 10.3390/w14050726.
2. Mao G., Han Y., Liu X., Crittenden J., Huang N., Ahmad U. M. Technology status and trends of industrial wastewater treatment: a patent analysis. *Chemosphere*. 2022. Vol. 288. p. 132483. DOI: 10.1016/j.chemosphere.2021.132483.
3. Piirainen V. Yu., Mikhailov A. V., Barinkov V. M., Starovoitov V. N. The use of sludge-peat composition for the processing of alumina production waste. *Obogashchenie rud*. 2022. No. 6. pp. 51–58.
4. Dutta D., Arya S., Kumar S. Industrial wastewater treatment: Current trends, bottlenecks, and best practices. *Chemosphere*. 2021. Vol. 285. pp. 131245. DOI: 10.1016/j.chemosphere.2021.131245.
5. Gendler S. G., Stepantsova A. Y., Popov M. M. Justification on the safe exploitation of closed coal warehouse by gas factor. *Journal of Mining Institute*. 2024. Vol. 271. pp. 1–11. EDN SIJDWE.
6. Karapetyan K. G., Dorosh I. V., Zgonnik P. V., Korshunov A. D., Perina A. I. Sorbents based on foamed phosphate glass for collecting petroleum oil products from contaminated soils and water surfaces. *Bulletin of the Tomsk Polytechnic University. Geo Assets Engineering*. 2024, Vol. 335. No. 8. pp. 227–240. DOI: 10.18799/24131830/2024/8/4484.
7. Alibabaei F., Saebnoori E., Fulazzaky M. A., Talaeikhozani A., Roohi P., Moghadas, F., Alian T. An evaluation of the efficiency of

odorant removal by sodium ferrate (VI) oxidation. *Measurement*. 2021. Vol. 179. p. 109488. DOI: 10.1016/j.measurement.2021.109488.
8. Kareem B. Y., Al Tameemi H. M. The performance of potassium ferrate for COD removal in AL-SAMAWAH refinery wastewataer. *AIP Conference Proceedings. Najaf, Iraq 22–23 March 2021*. 2022. Vol. 2386. No. 1. p. 080023. DOI: 10.1063/5.0066964.
9. Altynbayeva G., Kadnikova O., Aydarhanov A., Toretayev M. Industrial wastewaters of the feed industry: use of sodium ferrate in the phenol purification process. *Rigas Tehniskas Universitates Zinatniskie Raksti*. 2021. Vol. 25. No. 1. pp. 829–839. DOI: 10.2478/rtuect-2021-0062.
10. Sailo L., Pachuau L., Yang J. K., Lee S. M., Tiwari D. Efficient use of ferrate (VI) for the remediation of wastewater contaminated with metal complexes. *Environmental Engineering Research*. 2015. Vol. 20. No. 1. pp. 89–97. DOI: 10.4491/eer.2014.079.
11. Gunawan G., Haris A., Prasetya N. B. A., Pratista E., Amrullah A. Ferrate (VI) synthesis using $Fe(OH)_3$ from waste iron electrolysis and its application for the removal of metal ions and anions in water. *Indonesian Journal of Chemistry*. 2021. Vol. 21. No. 6. pp. 1397–1407. DOI: 10.22146/ijc.64824.
12. Dong S., Mu Y., Sun X. Removal of toxic metals using ferrate (VI): a review. *Water Science and Technology*. 2019. Vol. 80. No. 7. pp. 1213–1225. DOI: 10.2166/wst.2019.376.
13. Andreev S. Yu., Garkina I. A., Knyazev A. A., Dolgushev M. S. Study of the technological process of electrochemical synthesis of sodium ferrate in anode cells of a membrane electrolyzer. *Regional architecture and construction*. 2020. No. 2. pp. 142–149.
14. Petkova A. P., Gorbatyuk S. M., Sharafutdinova G. R., Nagovitsyn V. A. Selection of materials and technologies for the electrochemical synthesis of sodium ferrate. *Metallurgist*. 2024. Vol. 68. No. 3. pp. 449–459. DOI: 10.1007/s11015-024-01747-w.
15. Goodwill J. E., LaBar J., Slovikosky D., Strosnider W. H. Preliminary assessment of ferrate treatment of metals in acid mine drainage. *Journal of environmental quality*. 2019. Vol. 48. No. 5. pp. 1549–1556. DOI: 10.2134/jeq2019.02.0079.
16. Munyengabe A., Zvinowanda C., Ramontja J., & Zvimba J. N. Effective desalination of acid mine drainage using an advanced oxidation process: Sodium ferrate (VI) salt. *Water*. 2021. Vol. 13. No. 19. pp. 2619. DOI: 10.3390/w13192619.
17. Sarantseva A. A., Ivantsova N. A., Kuzin E. N. Investigation of the Process of Oxidative Degradation of Phenol by Sodium Ferrate Solutions. *Russian Journal of General Chemistry*. 2023. Vol. 93. No. 13. pp. 3454-3459. DOI: DOI 10.1134/s1070363223130273.
18. Sarantseva A. A., Astakhov P. S., Kuzin E. N. Study of the disinfectant capacity of sodium ferrate. *Occupational safety in industry*. 2024. No. 7. pp. 47-53. DOI 10.24000/0409-2961-2024-7-47-53.
19. Thomas M., Kozik V., Barbusiński K., Sochanik A., Jampilek J., Bak A. Potassium ferrate (Vi) as the multifunctional agent in the treatment of landfill leachate. *Materials*. 2020. Vol. 13. No. 21. pp. 5017. DOI: 10.3390/ma13215017.
20. Orekhova A. I., Khalemskiy A. M., Sherstobitova T. M., Kogan B. S. Purification of industrial waters of the Urals using a new oxidizing reagent. *Non-ferrous Metallurgy*. 2013. No. 4. pp. 64–67.
21. Vologzhanina S. A., Ermakov B. S., Ermakov S. B., Khuznakhmetov R. M. Relationship between operating conditions and the emergence of nano- and ultradispersed grain boundary defects in weld joints. *Tsvetnye Metally*. 2023. No. 8. pp. 80–85.
22. Sun X., Zhang Q., Liang H., Ying L., Xiangxu M., Sharma V. K. Ferrate (VI) as a greener oxidant: Electrochemical generation and treatment of phenol. *Journal of hazardous materials*. 2016. Vol. 319. pp. 130-136. DOI: 10.1016/j.jhazmat.2015.12.020.
23. Wang H., Liu Y., Zeng F., Song S. Electrochemical synthesis of ferrate (VI) by regular anodic replacement. *International Journal of Electrochemical Science*. 2015. Vol. 10. No. 10. pp. 7966–7976. DOI: 10.1016/S1452-3981(23)11069-8.
24. Diaz M., Doederer K., Keller J., Cataldo M., Donose B. C., Ali Y., Ledezma P. Towards in situ electro-generation of ferrate for drinking water treatment: A comparison of three low-cost sacrificial iron electrodes. *Journal of Electroanalytical Chemistry*. 2021. Vol. 880. p. 114897. DOI: 10.1016/j.jelechem.2020.114897.
25. Barışçı S., Ulu F., Särkkä H., Dimoglo A., & Sillanpää M. Electrosynthesis of ferrate (VI) ion using high purity iron electrodes: Optimization of influencing parameters on the process and investigating its stability. *International Journal of Electrochemical Science*. 2014. Vol. 9. No. 6. pp. 3099–3117. DOI: 10.1016/S1452-3981(23)07995-6.
26. Deng Y., Guan X. Unlocking the potential of ferrate (VI) in water treatment: Toward one-step multifunctional solutions. *Journal of Hazardous Materials*. 2024. Vol. 464. p. 132920. DOI: 10.1016/j.jhazmat.2023.132920.
27. Litvinenko V. S., Dvoynikov M. V., Trushko V. L. Elaboration of a conceptual solution for the development of the Arctic shelf from seasonally flooded coastal areas. *International Journal of Mining Science and Technology*. 2022. Vol. 32. No. 1. pp. 113–119. DOI: 10.1016/j.ijmst.2021.09.010.
28. Bazhin V. Y., Ustinova Y. V., Fedorov S. N., Shalabi M. E. K. Improvement of energy efficiency of ore-thermal furnaces in smelting of alumosilicic raw materials. *Journal of Mining Institute*. 2023. Vol. 261. pp. 384–391. EDN RTQXSE.
29. Mikhailov A. V., Shibanov D. A., Bessonov A. E., Bouguebrine C. Comprehensive Assessment Production Efficiency of Electric Rope Shovel through Operator Qualification Criteria. *Transactions A: Basics*. 2024. Vol. 37. No. 07. pp. 1231. DOI: 10.5829/IJE.2024.37.07A.03.
30. Petkova A. P., Sharafutdinova G. R. Justification of materials and technological parameters of sodium ferrate electrolysis process. *Design. Materials. Technology*. 2024. No. 2 (74). pp. 170–176. DOI: 10.46418/1990-8997_2024_2(74)_170_176.
31. Petkova A. P., Konyashina A. I., Sharafutdinova G. R. Development of the layout and manufacturing technology of a flow reactor for the electrochemical synthesis of sodium ferrate. *Design. Materials. Technology*. 2024. No. 3 (75). pp. 207–213. DOI: 10.46418/1990-8997_2024_3(75)_207_213.
32. Shulga E., Karamov R., S. Sergeichev I., D. Konev S., I. Shurygina L., S. Akhatov,I., G. Nasibulin A. Fused filament fabricated polypropylene composite reinforced by aligned glass fibers. *Materials*. 2020. Vol. 13. No. 16. pp. 3442. DOI: 10.3390/ma13163442.
33. Pryakhin E. I., Pribytkova D. A. The influence of the quality of surface preparation of pipes for heating networks on their corrosion resistance during operation in underground conditions. *Chernye Metally*. 2023. No. 11. pp. 97–102.
34. Korogodin A. S., Ivanov S. L. Assessment of the technical condition of drum mill supporting sliding bearings during operation as part of an arctic mining equipment complex. *Russian Mining Industry*. 2024. No. 6. pp. 144–151. DOI: 10.30686/1609-9192-2024-6-144-151.
35. Pryakhin E. I., Azarov V. A. Comparative analysis of the use of epoxy and fluoroplastic polymer compositions as internal smooth coatings of the inner cavity of steel main gas pipelines. *CIS Iron and Steel Review*. 2024. Vol. 28. pp. 93–98.
36. Feihu Z., Yi S. S. Electrochemical Synthesis of Ferrate (VI): Factors Influencing Synthesis and Current Research Trends. *Journal of Advanced Research in Applied Mechanics*. 2024. Vol. 117. No. 1. pp. 72–90. DOI: 10.37934/aram.117.1.7290.
37. Sun X., Zu K., Liang H., Sun L., Zhang L., Wang C., Sharma V. K. Electrochemical synthesis of ferrate (VI) using sponge iron anode and oxidative transformations of antibiotic and pesticide. *Journal of hazardous materials*. 2018. Vol. 344. pp. 1155–1164. DOI: 10.1016/j.jhazmat.2017.08.081.
38. Talaiekhozani A., Talaei M. R., Rezania S. An overview on production and application of ferrate (VI) for chemical oxidation, coagulation and disinfection of water and wastewater. *Journal of environmental chemical engineering*. 2017. Vol. 5. No. 2. pp. 1828–1842. DOI: 10.1016/j.jece.2017.03.025.
39. Belov B. F., Trotsan A. I., Brodetsky I. L., Kharlashin P. P., & Parenchuk I. V. Classification and optimization of ferrosilicon alloys. *New materials and technologies in metallurgy and machinery*. 2009. No. 2. pp. 129–133.
40. Čekerevac M. I. Investigation of electrochemical synthesis of ferrate, Part I: Electrochemical behavior of iron and its several alloys in concentrated alkaline solutions. *Hemijska industrija*. 2009. Vol. 63. No. 5. p. 387.